Technical Sciences
Academy of Romania
www.jesi.astr.ro

Journal of Engineering Sciences and Innovation
Volume 8, Issue 2/ 2023, pp. 159 - 170
http://doi.org/10.56958/jesi.2023.8.2.159

C. Chemical Engineering, Materials Science and Engineering

Received ***20 Apryl 2023*** *Accepted* ***26 June 2023***
Received in revised form ***21 June 2023***

Microstructures in as–cast condition of Medium Entropy Alloys designed to contain eutectic carbides TaC or HfC

NASSIMA CHENIKHA[1], PAULINE SPAETER[1], CORENTIN GAY[1], ANNE VERNIERE[1,2], PATRICE BERTHOD[1,2*]

[1]Faculté des Sciences et Technologies, Université de Lorraine, Campus Victor Grignard, 54500 Vandoeuvre–lès–Nancy, France
[2]Institut Jean Lamour, Université de Lorraine, Campus Artem, 2 allée André Guinier, 54000 Nancy, France

Abstract. Three alloys derived from the Cantor's CoNiFeMnCr equimolar composition, with a decreased Mn content and an increased Cr content, were cast to explore the possible microstructure changes induced by these composition modifications. One was a quinary alloy and the two other alloy result from the addition of either Ta and C, or Hf and C, to the previous one. As recently observed for an equimolar base, these addition of carbon and of the MC–former elements produced the interdendritic precipitation of eutectic script–like monocarbides, known to efficiently strengthen some cobalt–based superalloys at high temperatures. Enhanced creep resistance is thus expected, suggested here first by the increase in ambient temperature hardness, while improved high temperature oxidation resistance should be obtained by comparison to the equimolar CoNiFeMnCr a little too poor in chromium.

Keywords: Cantor–type MEA alloys, TaC carbides, HfC carbides, As–cast microstructure, XRD, Electron microscopy, Hardness.

1. Introduction

In the broad family of metallic materials, superalloys are among the most remarkable alloys thanks to their outstanding mechanical properties in a wide range of temperature [1,2]. Most of them are based on nickel or on cobalt, elements which can cause problems of low availability and high cost. Diluting Co and Ni among a wider list of base elements in a single alloy may partially solve these problems if earth–abundant and cheap elements as Fe or Mn are present instead a

*Correspondence address: patrice.berthod@univ-lorraine.fr

part of Ni and Co. Some resulting chemically complex alloys may be considered as High Entropy Alloys (HEA). Indeed, Co, Ni, Fe, Mn and Cr gathered in an alloy with significant quantities each, correspond to common examples of HEA [3]. A famous HEA involving these elements in identical molar contents is the Cantor alloy. Equimolar CoNiFeMnCr alloys can be elaborated by conventional foundry or following other elaboration techniques: single crystalline growth from liquid [4], additive manufacturing [5] or thin film development [6]. Well known for its mechanical properties from cryogenic temperatures to ambient temperature, the Cantor alloy can be also considered for uses at higher temperatures. It was recently demonstrated that promoting the formation of refractory carbides by addition of tantalum [7] or hafnium [8] in presence of carbon, interesting creep resistance can be achieved, even at 1100°C [9]. Unfortunately it was also seen that the oxidation resistance at such elevated temperature in air is not good. This was observed first metallographically after exposures in laboratory air at high temperature in furnaces [10], and second kinetically by applying thermogravimetry tests in synthetic dry air [11]. In both cases it appears that chromia was only a minor oxide to form while the major oxides were mixed oxides combining manganese and chromium, obviously much less protective than chromia.

To really benefit from the high temperature interesting creep resistance of these MC–reinforced HEA alloys it is compulsory to improve. Based on these previous observations concerning the probable deleterious effect of high content in manganese it was chosen to decrease the Mn content. Further, since the chromium content was itself a little too low (for obtaining a chromia–forming behavior, about 20wt.%Cr is required for Al–free Ni–based superalloys while this is near 30wt.% for Co–based superalloys) it was also decided to increase the Cr content. This double modification of the chemical compositions of the initial MC–strengthened Cantor alloys recently designed and investigated [7–11] is here experimented, with MC–alloys based on a now not–equimolar {Co, Ni, Fr, Mn, Cr} combination which is now more a Medium Entropy Alloy (MEA) [12] than a HEA one. The present work will present the obtained as–cast microstructures and phase compositions explored in electron microscopy imaging, X – ray diffraction and energy dispersion spectrometry. Additionally, indentation tests will give data about hardness and machinability, and first indications concerning the possibly improved high temperature oxidation and possibly modified creep behaviors will be communicated from the currently running experiments.

2. Methodology

To explore both the change in as–cast microstructure and hardness induced by the modifications in Mn and Cr contents as well as the specific effect of the presence of MC carbides for the new Mn–impoverished/Cr–enriched Cantor–type base, two compositions designed to promote one TaC–reinforcement and the second one Hf–reinforcement, as well as a third one which is carbide–free (no Ta, Hf and C), were elaborated. For the composition of the third alloy, playing the role of new reference

alloy, it was chosen to divide by 2 the Mn atomic content and to increase the Cr content by 50%. This alloy, which will be simply named "MEA", is thus a $CoNiFeMn_{0.5}Cr_{1.5}$ alloy. The first and second alloys, are both a $CoNiFeMn_{0.5}Cr_{1.5}$ one with added 0.25wt.%C and 3.77wt.%Ta for the former one (called "MEA/TaC"), and one with added 0.25wt.%C and 3.72 wt.%Hf for the later one (called "MEA/HfC"). These Ta and Hf weight contents were rated to respect the atomic equivalence between carbon and the carbide–forming metal to promote the formation of monocarbides, exclusively. The choice of 0.25wt.%C comes from the observations of the microstructures in as–cast condition 0.25wt.%C– and 0.50wt.%C–containing MC–strengthened Cantor–based alloys [7,8]. 0.50wt.%C was obviously too much since the carbides populations were too dense (threatened ductility and machinability) and the contents induced for Ta and Hf were high with as consequences high costs for the alloys. Further, too high contents in C and Hf led to important clusters of pre–eutectic HfC carbides in the microstructure, possibly deleterious for the properties of the alloy. On the other hand, 0.25 wt.%C appears as a minimum to obtain MC carbides in quantity high enough to produce significant alloy reinforcement against high temperature creep.

For each of these three new alloys, a procedure similar as what is described in [7,8] was followed:

- Accurate weighing of pure metals (Co, Ni, Fe, Mn, Cr: purity > 99.9%) and graphite (100%), bought by Alfa Aesar, Aldrich and Sigma, using a ±0.1mg precision balance;
- High frequency (≈100kHz) induction melting of the metals and graphite mixtures in a water–cooled copper crucible under inert atmosphere (300mbars of pure argon);
- Iso–voltage stage (≈5kV) for 15 minutes for complete melting and chemical homogenization of the liquid alloys;
- Cutting of the ingots (all weighing about 40 grams) using metallographic precision saw;
- Embedding of a cut part of each ingot in a cold resin – hardener mixture;
- Grinding (SiC papers from #240 to #1200) and polishing (sprayed 1 µm hard particles) until obtaining a mirror–like state;
- Microstructure exploration and imaging using a Scanning Electron Microscope (SEM; manufacturer: JEOL; model: JSM 6010LA) in Back Scattered Electrons (BSE) mode under 20kV (acceleration voltage);
- Chemical composition characterization using the Energy Dispersion Spectrometry (EDS) device attached to the SEM (full frame analysis for the chemical composition – except carbon – of the whole alloys, spot analysis of the matrix and of the other present phases, elemental mapping);
- X–ray diffraction (XRD) using a D8Advance diffractometer from Brüker (Cu Kα radiation, wavelength = 1.541 Angström);
- Vickers indentation (load 30kg).

3. Results and discussion

Obtained compositions

The chemical composition of the MEA alloy as measured with EDS full frame analysis is displayed in Table 1 (atomic contents) and Table 2 (weight contents). The atomic contents of Co, Ni and Fe are close to one another, and it is logically the same for their weight contents, taking into account that these elements have almost the same molar masses. The atomic and weight Mn contents are about half the Co, Ni and Fe ones, while the Cr contents are a half higher than the Co, Ni and Fe ones.

The compositions targeted for the MEA/TaC and MEA/HfC alloys were also successfully obtained. The contents in Ta and Hf are slightly overestimated because of the high concentrations in these elements in the carbides with tend emerging on surface after final polishing, because of their very high hardness.

Table 1. General chemical composition of the MEA alloy (average and standard deviation calculated from the results of four ×250 areas); all contents in atomic percent

MEA Full frame (at.%)	**Co**	**Ni**	**Fe**	**Mn**	**Cr**	**M**
Average	18.9	19.5	19.7	8.4	33.5	/
Standard deviation	0.1	0.3	0.2	0.5	0.4	/

Table 2. General chemical composition of the MEA alloy (average and standard deviation calculated from the results of four ×250 areas); all contents in mass percent

MEA Full frame (ms.%)	**Co**	**Ni**	**Fe**	**Mn**	**Cr**	**M**
Average	20.0	20.5	19.8	8.3	31.3	/
Standard deviation	0.1	0.3	0.18	0.5	0.4	/

Table 3. General chemical composition of the MEA/TaC alloy (average and standard deviation calculated from the results of four ×250 areas); all contents in weight percent, carbon not possible to analyze but supposed to be well respected: 0.25 wt.%C)

MEA/TaC Full frame (wt.%)	Co	Ni	Fe	Mn	Cr	Ta
Average	19.5	20.0	19.1	8.4	28.5	4.6
Standard deviation	0.2	0.5	0.3	0.2	0.3	0.2

Table 4. General chemical composition of the MEA/HfC alloy (average and standard deviation calculated from the results of four ×250 areas); all contents in weight percent, carbon not possible to analyze but supposed to be well respected: 0.25 wt.%C)

MEA/HfC Full frame (wt.%)	Co	Ni	Fe	Mn	Cr	Hf
Average	19.7	20.1	19.1	8.8	27.8	4.5
Standard deviation	0.4	0.3	0.3	0.3	0.7	0.6

As–cast microstructures as imaged with the SEM

The as–cast $CoNiFeMn_{0.5}Cr_{1.5}$ alloy ("MEA") is seemingly single–phased (uniformly gray) and no useful micrograph can be presented, as consequence. In contrast, SEM/BSE micrographs taken on the metallographic "MEA/TaC" and "MEA/HfC" alloys, which are multi–phased due to the presence of carbides, are of much higher interest. Their microstructures are each illustrated by a low magnification micrograph (general microstructure) and a high magnification one (detailed microstructure) in Figure 1. Obviously both alloys are dendritically structured (Figure 1, top), with the interdendritic spaces containing the MC carbides. The MC carbides are seemingly the single carbide phase present. The TaC carbides are of a single origin – precipitated during the eutectic part of the solidification (residual liquid → matrix + TaC) – as suggested by both their interdendritic location and their morphologies (closely imbricated with matrix). The HfC are obviously of two natures: eutectic carbides as TaC (for the same reasons), and pre–eutectic carbides formed prior to, or in parallel with, the dendritic development of the matrix. These later carbides appears as blocky particles gathered as clusters. Evidently, no chromium carbide precipitated at solidification, despite the increase in chromium content compared with the initial equimolar versions of these alloys [7,8], and these two alloys remain double–phased {matrix + MC}, which is promising for good mechanical resistance at elevated temperature. Concerning the apparent carbide fractions they are similar to

the ones in the initial equimolar versions [7,8], however with perhaps a slightly less dense TaC population and a little more dense HfC population for the present alloys than for the initial ones [7,8].

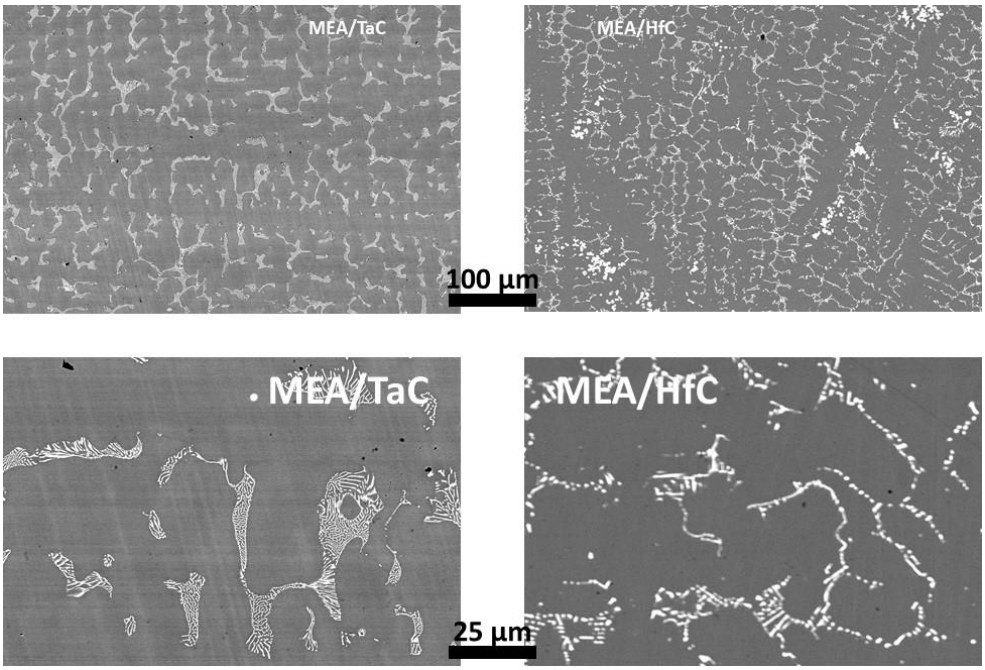

Fig. 1. SEM/BSE micrographs for general view (top) and detailed view (bottom) of the as–cast microstructures of the MEA/TaC (left) and MEA/HfC (right) alloys.

As–cast microstructures according to XRD

The X–ray diffraction runs have led to the diffractograms presented in Figure 2 for the MEA alloy, Figure 3 for the MEA/TaC alloy and Figure 4 for the MEA/HfC alloy. This confirms, first that the MEA alloy is really single–phased, and second that its single phase is austenitic (face centered cubic network). The matrixes of the MEA/TaC and MEA/HfC alloys are austenitic too, and the carbides present in these two later alloys are exclusively the monocarbides TaC and HfC, respectively. These XRD results, almost identical to the previous ones obtained for the initial equimolar versions [7,8], show that here too that the decrease in Mn and increase in Cr did not affect the natures of the phases present in the as–cast microstructures.

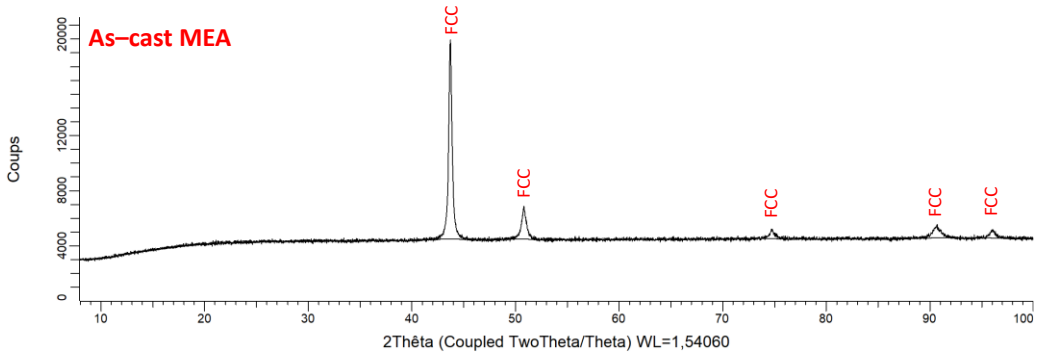

Fig. 2. Diffractogram acquired on the MEA alloy.

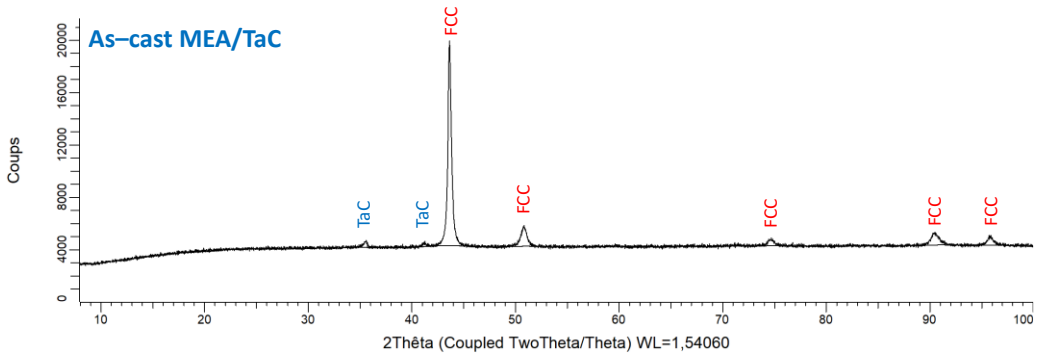

Fig. 3. Diffractogram acquired on the MEA/TaC alloy.

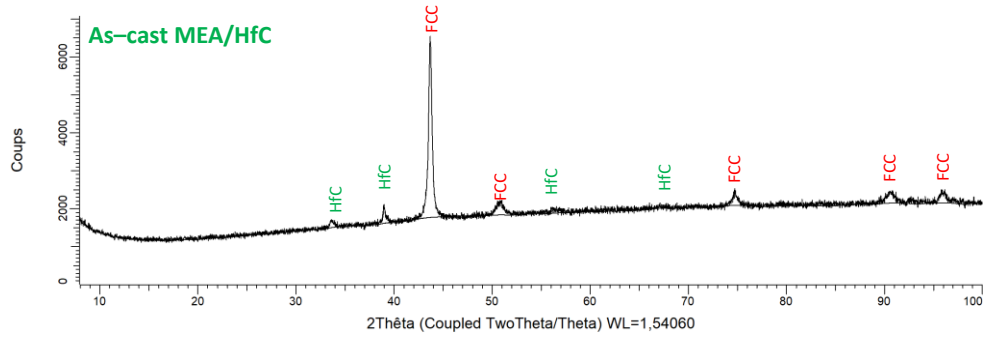

Fig.4. Diffractogram acquired on the MEA/HfC alloy.

As–cast microstructures according to EDS elemental mapping

The X–maps run on the MEA alloy (Figure 5) allow evidencing that this alloy is not chemically homogeneous in its as–cast state. Indeed, positive segregation of manganese obviously occurred during solidification, this resulting in locally high Mn concentration in the las zones to solidify (borders of solidification cells). In

these Mn–enriched intercellular zones the contents in all the four other elements are a mechanically little lower than in the cells themselves. These gaps in Co, Ni, Fe and Cr are individually logically less marked than the Mn enrichments. On can note that the distribution of Mn is useful to visualize the cells, the existence of which are thus demonstrated (instead dendrites), and to have an estimation of the average grain size (about 50 μm) as well as of their possible "granulometric" distribution in the ingot (between its center and its peripherical zones).

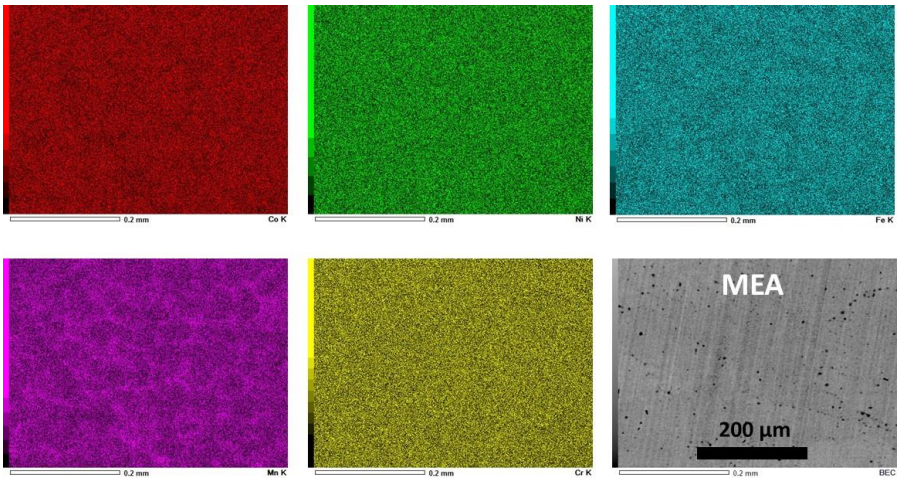

Fig. 5. EDS elemental mapping performed on the MEA alloy.

The same Mn segregation phenomenon took place also for the MEA/TaC (Figure 6) and MEA/HfC (Figure 7) alloys but it is much less visible. This is the presence of TaC or HfC carbides which induced the most visible heterogeneity of the alloys in Co, Ni, Fe and Cr the contents of which are much lower there, logically.

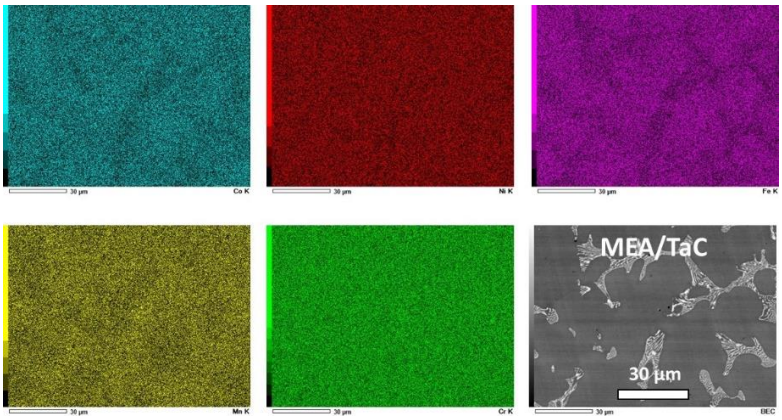

Fig. 6. EDS elemental mapping performed on the MEA/TaC alloy (Ta and C excepted).

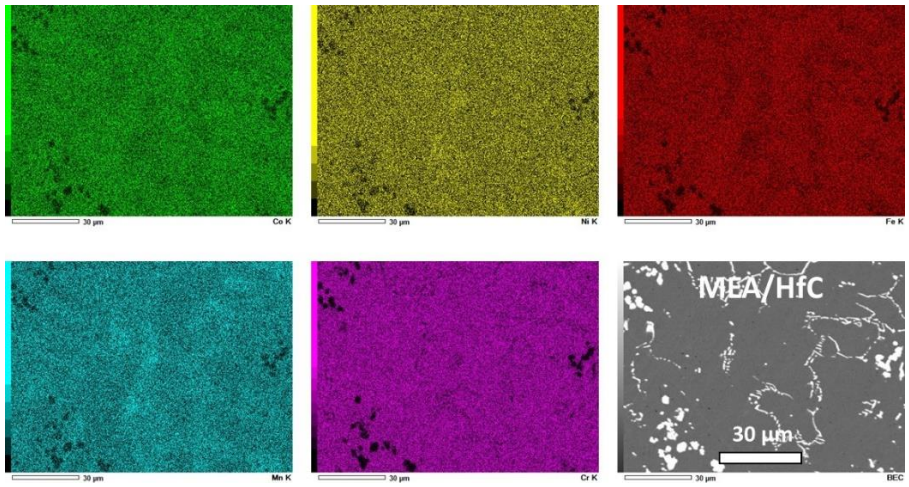

Fig .7. EDS elemental mapping performed on the MEA/HfC alloy (Hf and C excepted).

The case of the carbides is especially examined by the X–maps presented in Figure 8. The distributions of tantalum (respectively Hf) is very heterogenous in the microstructure of the MEA/TaC alloy (resp. MEA/HfC alloy), because the logically high concentration of these elements where the carbides are. This is the same for carbon that it is possible to see high centration where the coarse pre–eutectic HfC carbides are, but not for the eutectic carbides (TaC and HfC) which are too fine to allow any evidence of this too light element.
Another remarkable observation that can be done in Figure 8 is the presence in loo quantity of tantalum in the matrix of the MEA/TaC alloy while hafnium seems not existing in the matrix of the MEA/HfC alloy.

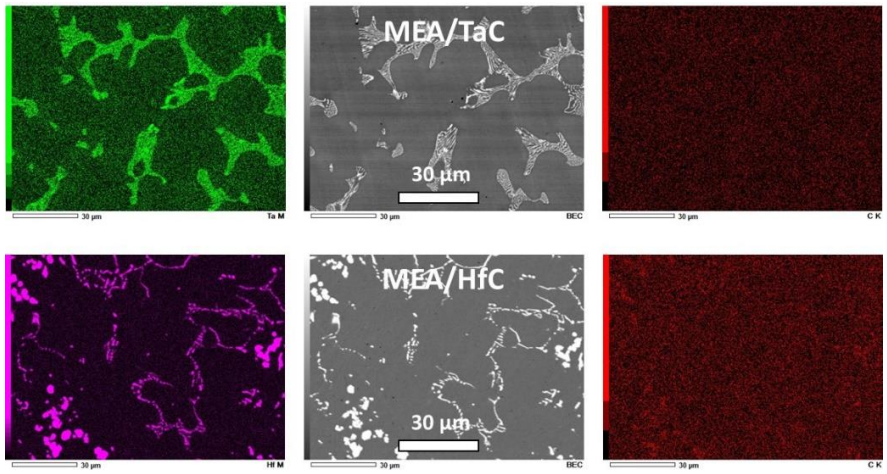

Fig. 8. EDS elemental mapping performed on the MEA/TaC and MEA/HfC alloys (only Ta, Hf and C).

Chemical composition of the matrixes

The previous observation concerning the presence or not of the MC–forming metal in solid solution in the matrix incites to measure the chemical composition of the matrix of each carbide–containing MEAs. The results displayed in Table 5 (MEA/TaC) and Table 6 (MEA/HfC) are the ones of spot analyses performed in the center of the dendrites. The contents in Co, Ni, Fe and Cr are globally the same as in the whole alloys. The Mn content is slightly lower than at the whole alloy scale, which can be easily explained by the segregation in manganese during solidification and the accumulation of this element in the interdendritic spaces. It appears too that a part of tantalum is stored in solid solution in the matrix (about 2.5 wt.%Ta) while Hf does not exist in the matrix (*the average value of 0.9 wt.%Hf results from the intersection of the interaction peer and subjacent HfC, which explains also the high standard deviation value). This observation concerning the presence of Ta and absence of Hf in the matrix is not surprising since it was earlier observed in TaC–containing Cr–rich Co–based [13], Ni–based [14] and Fe–based [15] alloys with the same C and Ta contents (0.2–0.25 wt.%C and 3–3.7 wt.%Ta). Concerning hafnium, the same absence of Hf in the matrix of the same types of alloys as above but with Hf instead Ta, was noticed whatever the base element too: Co [16], Ni[17] or Fe [18].

Table 5. Chemical composition of the matrix of the MEA/TaC alloy (average and standard deviation calculated from the results of four spot analyses); all contents in weight percent, carbon not possible to analyze but supposed present with extremely low contents.

MEA/TaC Spot/matrix (wt.%)	Co	Ni	Fe	Mn	Cr	Ta
Average	20.9	20.3	20.9	7.9	27.6	2.4
Standard deviation	0.4	0.3	1.5	0.9	0.9	0.5

Table 6. Chemical composition of the matrix of the MEA/HfC alloy (average and standard deviation calculated from the results of four spot analyses); all contents in weight percent, carbon not possible to analyze but supposed present with extremely low contents
(*: subjacent HfC partly present in the interaction peer).

MEA/HfC Spot/matrix (wt.%)	Co	Ni	Fe	Mn	Cr	Hf
Average	20.7	21.0	20.8	7.9	28.7	0.89*
Standard deviation	0.9	0.7	1.3	0.6	0.8	1.6*

Hardness

The five Vickers indentations carried out on each alloy led to the results displayed in Table 7. They show that none of the three alloys is very hard but also that the

presence of the carbides induced a significant hardening about 50HV30kg points more by comparison with the MEA alloy. Further, the results seems showing that the transition from the initial equimolar CoNiFeMnCr HEA base [7,8] to the $CoNiFeMn_{0.5}Cr_{1.5}$ MEA one, does not induce any change in hardness (124±2 for MEA against 121±2 for HEA, 180±4 for MEA/TaC against 180±4 for HEA/TaC, and 160±3 for MEA/HfC against 157±12 for HEA/HfC). In the other hand, one must highlighting that TaC are more efficient in hardness increase that HfC. One can suspect that it is because of a significant part of the produced HfC is obtained as compact blocky coarse particles which did not allow developing an interdendritic MC network as dense as in the MEA/TaC and HEA/TaC alloys, carbide skeleton able to resist more to the indentor penetration.

Table 7. Hardness of the MEA, MEA/TaC and MEA/HfC alloys.

Hardness (HV30kg)	**MEA**	**MEA/TaC**	**MEA/HfC**
Average	124.1	179.7	160.0
Standard deviation	1.9	3.5	3.0

4. Conclusion

The Cantor–based HEAs strengthened by either TaC or HfC recently demonstrated very promising creep resistance over the [1000, 1100°C] temperature range but bad oxidation behavior at the same temperature levels. This is what motivated this work consisting at first checking the possible influence of the content changes for Mn and Cr, the species which had showed the greatest influence (respectively: deleterious and beneficial) on the oxidation phenomena and kinetics. Obviously, the decrease in Mn and increase in Cr with the amounts tested here did not have any influence on the microstructures and the hardness. This led us to start controlling the general high temperature behavior of these MC–reinforced MEA alloys. In this on–going investigation, running creep tests (at 1000 and 1100°C under 20 MPa) tend showing that neither weakening nor strengthening may result from these Mn decrease and Cr increase [19]. Concerning high temperature oxidation, some preliminary results (at 1000 and 1100°C for 50h in synthetic air) seem demonstrating that these Mn decrease and Cr increase lead to significant improvement the oxidation behavior, as expected [20]. For instance, the mass gains after 50 hours are between 2 times and 4 times lower for the quinary and MC–strengthened MEAs than for the equivalent HEAs. This confirms the interest to modify the initial Cantor's composition in the ways explored here, to possibly adapt the composition of this alloy interesting for ambient and low temperatures for applications at the temperatures of service of superalloys.

Acknowledgments

The authors wish to thank Mr. Erwan Etienne for his technical help for cutting and polishing, and Ghouti Medjahdi for his help for the X–ray diffraction runs.

References

[1] Sims C.T., Stoloff N.S., Hagel W.C., *Superalloys II. High Temperature Materials for Aerospace and Industrial Power*, John Wiley & Sons, 1987.
[2] Donachie M.J., Donachie S.J., *Superalloys: A Technical Guide* (2nd edition), ASM International, 2002.
[3] Liu S.F., Wu Y., Wang H.T., He J.Y., Liu. J.B., Chen C.X., Liu X.J., Wang H., Lu Z.P., *Intermetallics*, **93**, p. 269–273.
[4] Kawamura M., Asakura M., Okamoto N. L., Kishida K., Inui H., George E.P, *Acta Materialia*, **203**, 116454, 2021.
[5] Osintsev K., Konovalov S., Zaguliaev D., Ivanov Y., Gromov V., Panchenko I., *Metals*, **12**, 197, 2022.
[6] Hu M., Cao Q.P., Wang X.D., Zhang D.X., Jiang J.Z., *Metals*, **12**, 197, 2022.
[7] Berthod P., *Journal of Metallic Materials Research*, **5**, 2022, p. 1–10.
[8] Berthod P., *Journal of Engineering Sciences and Innovation*, **7**, 2022, p. 305–314.
[9] Berthod P., *Proceeding of the 152nd Annual Meeting of The Minerals, Metals & Materials Society (TMS 2023)*, p. 1103–1111, 2023.
[10] Berthod P., *Proceeding of the 152nd Annual Meeting of The Minerals, Metals & Materials Society (TMS 2023)*, 2023, p. 933–941.
[11] Berthod P.; *Materials and Corrosion*, On-line first, 2023. DOI:10.1002/maco.202213721.
[12] Bracq G., Laurent-Brocq M., Varvenne C., Perrière L., Curtin W.A., Joubert J. M., Guillot I., *Acta Materialia*, **177**, 2019, p. 266–279.
[13] Michon S., Berthod, P., Aranda L., Rapin C., Podor R.; Steinmetz P., *Calphad*, **27**, p. 289–294, 2003.
[14] Berthod P., Aranda, L., Vébert C., Michon S., *Calphad*, **28**, 2004, p. 159–166.
[15] Berthod P., Hamini Y., Aranda L., Héricher L., *Calphad*, **31**, 2007, p. 351–360.
[16] Conrath E., Berthod P., *Corrosion Engineering, Science and Technology*, **49**, p.45–54, 2014.
[17] Berthod P., Conrath E., *Materials at High Temperatures*, **31**, 2014, p. 266–273.
[18] Berthod P., Conrath E., *Oxidation of Metals*, **82**, 2014, p. 33 – 48.
[19] Gay C., Chenikha N., Spaeter P., Etienne E., Vernière A., Aranda L., Berthod P., *Indonesian Journal Of Innovation And Applied Sciences*, to be submitted.
[20] Spaeter P., Gay C., Chenikha N., Vernière A., Medjahdi G., Aranda L., Berthod P., *Corrosion and Materials Degradation*, to be submitted.